UNIVERSIDAD
NACIONAL
DE COLOMBIA

Genesis and Evolution of Pegmatites in Eastern Colombia: Insights from Mineral Chemistry

Estefany Andrea Mora-Galindo[1], Juan Carlos Molano Mendoza[1], Milton Julián Morales[2]

1. Universidad Nacional de Colombia
2. Servicio Geológico Colombiano

*Corresponding author: eamorag@unal.edu.co

ABSTRACT

Pegmatites and granitic intrusives from eastern Colombia, belonging to the Guainía department, were studied to determine the generating magma type, as well as to assess the degree of magmatic fractionation and its relationship with the presence of Nb-Ta-bearing minerals (strategic minerals). To that end, 31 rock samples were studied; EPMA electronic microprobe analyses were conducted on apatite, biotite, garnet, microcline, muscovite, and tourmaline. The results from biotite, garnet, and tourmaline suggest that these rocks originated from a Fe-rich peraluminous melt.

Moreover, content variation of Ba in microcline, Na in muscovite, Fe-Mg in biotite, and Mn-Sr in apatite, allowed the proposal of a magmatic evolutionary line for these rocks. Nb-Ta-bearing samples were present in the most fractionated rocks where tourmaline and garnet occurred, and thus, were proposed as possible indicators of strategic minerals.

Génesis y evolución de pegmatitas en el oriente colombiano mediante química mineral

RESUMEN

Se estudiaron pegmatitas e intrusivos graníticos del este de Colombia pertenecientes al departamento del Guainía para determinar el tipo de magma generador, su grado de fraccionamiento magmático y su relación con la presencia de minerales portadores de Nb-Ta (minerales estratégicos). Con este propósito, se estudiaron 31 muestras de rocas y se realizaron análisis con microsonda electrónica EPMA en apatito, biotita, granate, microclina, muscovita y turmalina. Los resultados obtenidos a partir de biotita, granate y turmalina sugieren que dichas rocas se generaron a partir de un magma peraluminoso rico en Fe.

Además, la variación del contenido de Ba en la microclina, Na en la muscovita, Fe-Mg en la biotita, y Mn-Sr en el apatito permitió proponer una línea evolutiva magmática para estas rocas. Las muestras portadoras de Nb-Ta estaban presentes en las rocas más fraccionadas, donde se encontraron turmalina y granate, por lo que se propusieron como posibles indicadores de minerales estratégicos.

1. Introduction

In eastern Colombia, rocks belonging to the Guainía department have been identified as having economic potential in strategic minerals (Franco et al., 2021a; Lopez & Cramer, 2014).

This motivated a research agreement between the Universidad Nacional de Colombia and the Servicio Geológico Colombiano (Colombian geological service) where granitic and pegmatitic samples were collected in the eastern border of the Guainía Department, in the surroundings of San Jose, Macanal, and Tabaquén (Guerrero et al., 2017; Morales et al., 2017; Zarate et al., 2017). However, the persistent lack of certainty regarding the magma type that formed such granites and pegmatites, their interrelations, and that with the presence of Nb-Ta-bearing minerals (Bayona-Valderrama, 2018; Charry et al., 2023) motivated the present study. With this aim, major, minor, and trace elements were analyzed in apatite, biotite, garnet, microcline, muscovite, and tourmaline.

In particular, the utility of biotite was examined, both to correlate these pegmatitic bodies to a generating magma type (Nachit, 1985; Stussi & Cuney, 1996), and together with the trace element analysis of microcline and muscovite, to determine the degree of fractionation of the intrusives (Alfonso et al., 2003; Černý et al., 1985; London et al., 1990).

Furthermore, elemental analysis of apatite, garnet, and tourmaline were conducted to supplement the information obtained from the previous minerals. These analyses contribute to the understanding of both the petrogenetic evolution and the type of magma involved in these processes.

Finally, the interrelation between the presence of Nb-Ta-bearing minerals and translucent minerals was evaluated as an exploration vector.

2. Geological context

2.1 Regional geological context

Eastern Colombia exposes part of the Amazon Craton, which has been subdivided into the following geochronological provinces (from oldest to newest): Central Amazonic (> 2.3 Ga), Maroni-Itacaiunas (2.2–1.95 Ga), Venturi-Tapajós (1.95–1.80 Ga), Rio Negro-Juruena (1.8–1.55 Ga), Rodonian-San Ignacio (1.55–1.3 Ga) and Sunsás (1.3–1.0 Ga) according to Tassinari and Macambira (1999) (Fig. 1).

Of the above, the one extending over the eastern part of Colombia (Fig. 2), and therefore the study area, is the Río Negro-Juruena province, with a total extension of approximately 2000 km in the NW-SE direction, and 600 km in the NE-SW direction (Tassinari & Macambira, 1999). According to these authors, this province mainly consists of granite gneisses, tonalitic, and granodiorite granitoids, with ages ranging between 1.8-1.50 Ga where ages decrease toward the western margin (Cordani et al., 2016).

Cordani et al. (2016) divided the NW fraction of the Rio Negro-Juruena Province in the Atabapo and Vaupes belts, using U-Pb (zircon), Sm-Nd (model ages), and Rb-Sr (whole-rock) isotope analysis, and a compilation of previous U-Pb (zircon and monazite) K-Ar (micas) and Rb-Sr (whole-rock and micas) dating.

- The Atabapo Belt ranges from 1.80 Ga to 1.74 Ga. During this period formed its basement, which corresponds to a series of magmatic arc orogenic pulses. Subsequently, it was intruded by granitic bodies (1.50 Ga) (Fig. 2).
- The Vaupes Belt formed between 1.58 Ga and 1.50 Ga by a series of orogenic pulses with magmatic arc affinity (Brito Neves, 2011). This agrees with the report of syntectonic calco-alkaline gneisses and migmatites in mid-amphibolite facies by Priem et al. (1982). In addition, Cordani et al. (2016) reported younger undeformed granite rocks, which could be posterior to the formation of this belt (Fig. 2).

Bonilla et al. (2021) presented concurring evidence for the evolution of the Rio Negro-Juruena Province. In Guainía, Colombia, ages between 1.85 and 1.72 Ga were associated to metamorphic and igneous rocks belonging to the Mitu Complex. These ages were interpreted by these authors as a result of the Statherian collisional and orogenic events (i.e., the Querari Orogeny). Furthermore, Bonilla et al. (2021) identified additional orogeny-related rocks

ranging 1.60 to 1.50 Ga old. Such results can be related to the Atapabo Belt and Vaupes Belt of Cordani et al. (2016), respectively. It is worth noting that, although some authors prefer using the term "Mitu Complex" due to its heterogeneous nature, the officially recognized name for this unit is the "Migmatitic Mitu Complex" (Rodriguez et al. 2011).
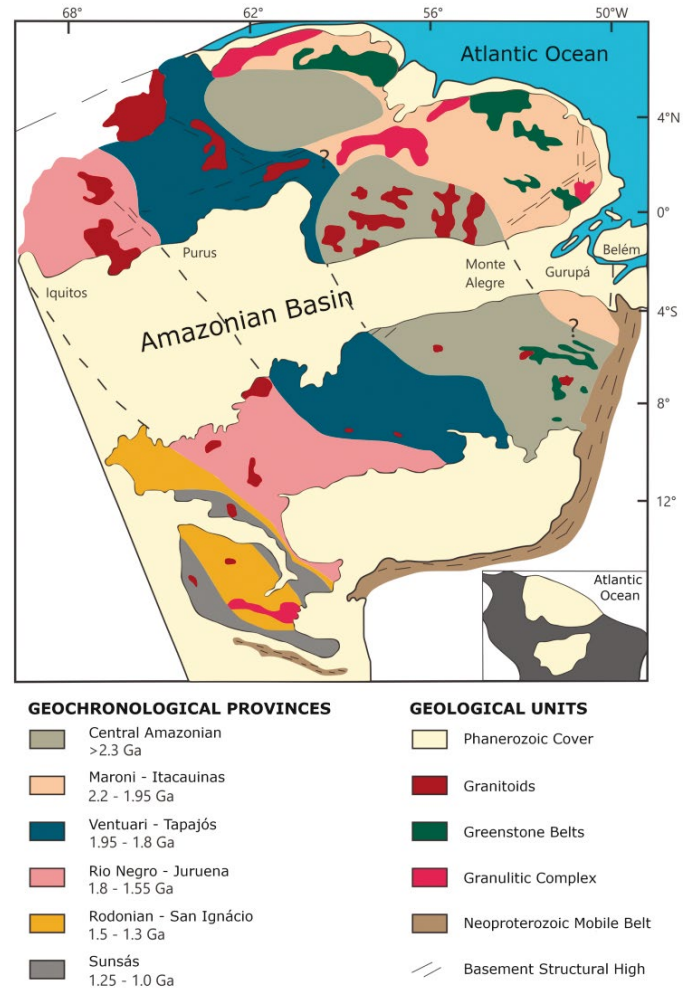

Figure 1. Geochronological provinces in the Amazon Craton. Region of interest is shown in a dashed rectangle. Modified from Tassinari and Macambira (1999).

According to Cordani et al. (2016), the interval between the formation of these belts allowed the cratonization of the Atabapo Belt and the intrusion of granite bodies as a reflection of the orogenic pulse that formed the Vaupes Belt. Bonilla et al. (2021) reported decompressional melting in the Guainía and Vaupes departments, resulting in the formation of A-type granites with LA-ICP-MS zircon U-Pb ages dating from 1.40 to 1.34 Ga. These authors suggest that the Matraca Granite in Guainía can be correlated with the Parguaza intrusion in Venezuela, crystallizing during a later phase of that event. Furthermore, a recent apatite LA-ICP-MS U-Pb geochronology study identified two stages of anorogenic events in eastern Colombia. The first occurred between 1.55-1.40 Ga, followed by the second stage between 1.40-1.34 Ga. These events were associated with ore deposits of incompatible elements, including Nb, Ta, REE, and U (Bonilla et al. 2023).

Regarding the São Gabriel-Içana River area (Fig. 2), Sr isotopic redistribution was found in association with ages of 1203 ± 58 Ma (Cordani et al., 2016), a fact that could correspond to the high-grade metamorphism that occurred during accretion of the Sunsás province (Tassinari & Macambira, 1999).
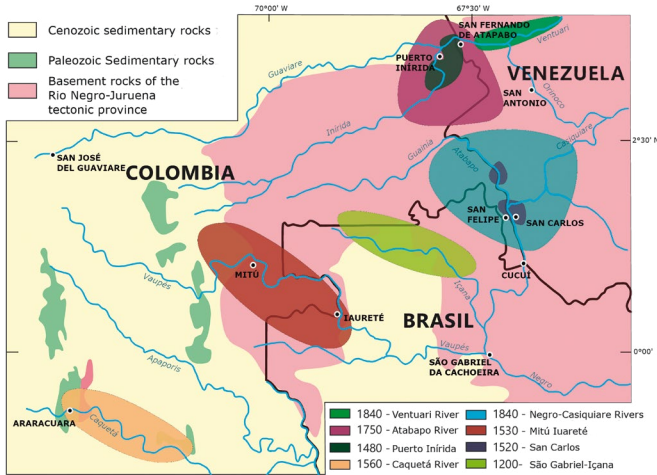
Figure 2. Geochronological belts as proposed by Cordani et al. (2016) on the border between Colombia, Venezuela, and Brazil. Modified from Cordani et al. (2016)

2.2 Local geological context

In Colombia, the rocks of the Rio Negro-Juruena Province have not been as exhaustively studied as those in the Cordillera, primarily owing to its remoteness and the characteristic dense vegetation of this tropical region.

However, rock samples were collected within an area of 198 Km^2 (Guerrero et al., 2017), between the Tabaquén and Macanal indigenous communities along the Guainía River (Fig. 3). This area has dense vegetation, high temperature and moisture levels, and a smooth relief with an average slope of 1.3% along the Guainía River.
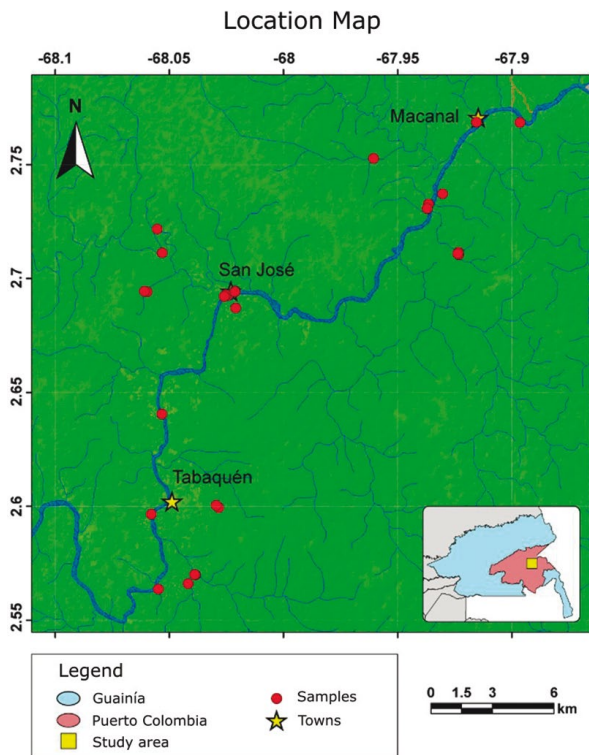

Figure 3. Location of study area and samples in the department of Guainía. Modified from Charry et al. (2023).

Mainly granitic intrusives, gneiss, pegmatite dykes, and quartz veins were found. A more detailed field characterization allowed to identify syenites, syenite quartz, monzonite quartz, granites, and granodiorites among the intrusive bodies. These rocks had textures ranging between equigranular and inequigranular, and the predominant colorations were white, light gray, and light brown (Fig. 4C). The most common accessory minerals were biotite, amphibole, and magnetite with slight orientation for some of the crystals. These rocks are cut by pegmatite dikes with thicknesses between 2 cm and 4.5 m and show net to transitional contacts (Guerrero et al., 2017) (Fig. 4D, E, F). Quartz veins in stockwork arrangements were found as well.

The composition of the pegmatites resembled that of the granitoids they intrude and had no clear internal zonation. This has been interpreted as a possible genetic relationship between them. In addition, some metamorphic rock outcrops such as granite orthogneiss and paragneiss (Fig. 4B) were found.

A striking feature was the presence of schorl tourmaline associated both with the paragneisses and quartz veins (Morales et al., 2017); such crystals' size reached up to 3 cm and were oriented 0° to 45° with respect to foliation (Fig. 4A).

Furthermore, pan concentrates samples were taken in this expedition, where Nb-rutile (also known as ilmenorutile) was found along with columbite and some strüverite grains intergrowth (Zarate et al., 2017).
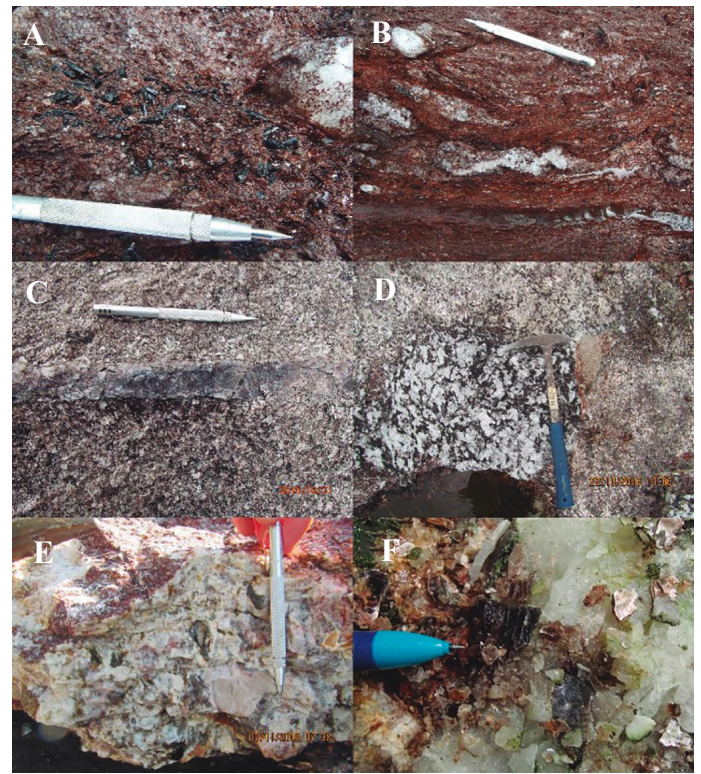

Figure 4. Outcrop photographs (A, B, C, D) and hand samples (E, F). A and B: Paragneiss N_2816, the black crystals in photograph A correspond to tourmalines. C: Granitic intrusive (two-feldspar granite) cut by quartz vein GV_2861. D: Pegmatitic enclave outcrop P_2846. E: Pegmatite hand sample P_2984. F: Pegmatite sample P_2883.

It is important to note that Nb-Ta-bearing minerals have been reported in the study area (Zarate et al., 2017) and in the neighboring anorogenic igneous body, the Parguaza Granite (Bonilla-Perez et al., 2013; Gonzalez & Pinto, 1990). This intrusive has been associated with Nb-Ta mineralizations (Bangerter, 1985; Franco et al., 2021a) which include cassiterite, struverite, tantalite-columbite, and ixiolite in pegmatites and quartz veins (Aarden & Davidson, 1978; Gaudette et al., 1978; Rodriguez & Perez, 1982).

Methodology

Out of the rock samples, 31 polished thin sections were made including granitic intrusives, pegmatite dykes, quartz veins, and one paragneiss. Petrographic analysis by optical microscopy was performed in all of them (see Results). A subsequent selection of the samples was made according to their quality; high quality meant the least possible presence of hydrothermal and/or supergene alterations to ensure reliable results in the EPMA analysis. This resulted in 23 samples of which 1 corresponded to a paragneiss (N), 8 to granitic intrusives (G) from which 3 were cut by quartz veins (GV), and 14 to pegmatitic bodies (P) (including dykes, lenses, and Qz-rich rocks with pegmatitic texture).

3.1 Analytical methods

Between two and three points per crystal (taken from center to the edge) were analyzed using an EPMA electronic microprobe (JEOL JXA-8230), resulting in a total of 254 measurement points on 93 crystals from 23 polished thin sections.

The instrument was operated in all cases with natural standards in WDS (wavelength-dispersion spectroscopy) mode, with graphite coating, and a voltage of 15 keV. Table 1 shows both the measurement parameters and the chemical elements analyzed in biotite. For measurement parameters of apatite, garnet, microcline, muscovite, and tourmaline refer to Appendix A.

Microcline, muscovite, and biotite crystals were selected in all thin sections, except in those where such crystals were absent or altered (Table 2). Some of these minerals were in paragenesis with opaque minerals, which were analyzed by Bayona-Valderrama (2018) and Charry et al. (2023) using EPMA electron microprobe and Raman spectroscopy. According to these authors, those minerals were magnetite, hematite, ilmenite, Nb-rutile, and columbite (Table 2); the last two define hereafter the Nb-Ta bearing samples, which are highly relevant to the fractionation degree discussion. It is worth noting that these minerals presented Ta_2O_5 contents, between 1.78-6.05 wt% for Nb-rutile, and between 5.29-6.05 wt% for columbite (Bayona-Valderrama, 2018).

Only the crystals comprising a primary magmatic mineral assemblage were selected. However, some crystals that seemed to indicate later introduction were selected as well (Table 2). On the other hand, those included in other crystals were not considered to ensure analyzing the highest state of evolution reached by the rock.

Representative crystals were chosen when significant textural changes were visible within a sample. Additionally, tourmaline, garnet, and apatite crystals were included to supplement the information obtained from the other minerals (Table 2).

Table 1. EPMA analysis conditions for biotite

Biotite										
Analyzed element (radiation line)	Si (Kα)	Ti (Kα)	Al (Kα)	Cr (Kα)	Fe (Kα)	Mn (Kα)	Mg (Kα)	Ca (Kα)	Na (Kα)	K (Kα)
Detection limit (ppm)	62	36	34	43	48	43	33	23	35	19
Diffraction crystal	1 TAP	3 PETH	1 TAP	3 LIFH	3 LIFH	3 LIFH	1 TAP	3 PETH	1 TAP	3 PETH
Counting time (peak)[s]	30	30	30	30	30	30	30	30	10	30
Counting time (background) [s]	15	15	15	15	15	15	15	15	10	15
Standard	Kyanite	Ilmenite	Orthoclase	Chromite	Almandine	Spessartine	Hornblende_143965	Anortite	Albite	Hornblende_143965
Beam current (nA)	20	20	20	20	20	20	20	20	20	20

Table 2. Relationships of the microprobe-analyzed minerals and associated opaque minerals. The column "In paragenesis" presents those opaque minerals that were in paragenesis with the analyzed mineral.

Sample	Analyzed minerals	Opaque minerals*		Observations
		In paragenesis	Others present in sample	
N_2816	Tourmaline			Possible association with pegmatites
G_2895	Apatite			
G_2973	Biotite			
G_2937	Biotite			Mineral is possibly part of a late event
G_2936	Muscovite	Magnetite	Magnetite, Ilmenite	Rock with high biotite content
	Microcline	Magnetite		
	Biotite			
	Apatite	Magnetite, Ilmenite		

(Continued)

Sample	Analyzed minerals	Opaque minerals*		Observations
		In paragenesis	Others present in sample	
G_3003	Microcline			
	Biotite			Measured points are part of a possible late event
	Apatite			
GV_2861	Muscovite	Magnetite, Ilmenite	Hematite, Magnetite, Ilmenite	
	Microcline			
	Tourmaline			Borders quartz vein that cuts the intrusive (sample)
GV_3012	Muscovite			
	Microcline			
	Biotite			
GV_2815	Tourmaline			Borders quartz vein that cuts the intrusive (sample)
P_2870	Muscovite			
	Microcline	Magnetite		
	Biotite			
P_2807	Muscovite	Ilmenite, Magnetite	Ilmenite	Thin section presents a contact between pegmatitic and mesogranular texture
	Microcline	Ilmenite		
	Tourmaline			
P_2917	Muscovite			Mineral is possibly part of a late event
	Microcline			
	Tourmaline			
P_2972	Muscovite	Ilmenite	Magnetite, Ilmenite	
	Microcline			
	Biotite	Magnetite		
P_2820	Muscovite	Magnetite	Ilmenite	Measured points are part of a possible late event
P_2846	Muscovite	**Nb-rutile**	**Columbite, Nb-rutile,** Magnetite	
	Microcline			
P_2883	Muscovite	Magnetite, Ilmenite	**Nb-rutile**	
	Microcline	**Nb-rutile**		
P_2984	Muscovite			
	Microcline			
	Biotite			
P_2995	Microcline	**Columbite**, Ilmenite, Hematite		
P_3005	Muscovite			
	Microcline			
P_3006	Muscovite			
	Microcline			
	Garnet			
P_2823	Muscovite	Magnetite		
P_2940	Microcline			
	Tourmaline			
P_2935	Muscovite			
	Microcline			
*In bold, strategic minerals analyzed by Bayona-Valderrama (2018) and Charry et al. (2023)				

4. Results

4.1 Petrographic analysis

Paragneiss

N_2816:

This rock mainly consisted of quartz, muscovite, and biotite, with clear orientation of the crystals, and micas-quartz micro-banding. Some euhedral to subhedral tourmaline crystals were found, and some of them were concordant with the foliation of the rock (Fig. 5).
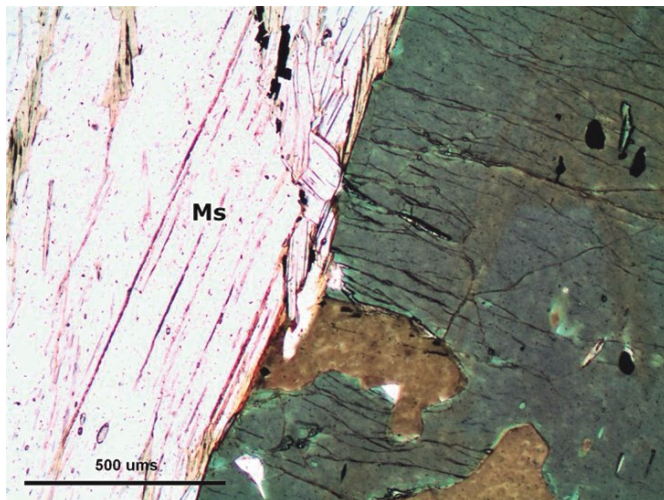

Figure 5. PPL Microphotograph of gneiss. Muscovite crystals in paragenesis with some opaque crystals and a tourmaline crystal covering the right portion of the photo.

Granitic intrusives

These samples presented textural variation between fine and coarse, and in some cases crystals larger than 1 cm. The predominant minerals were quartz, with lower content of plagioclase (albite to oligoclase) than microcline and variable content of biotite and muscovite.

Plagioclase, as opposed to microcline, was generally altered. Apatite, zircon, magnetite, and ilmenite were also identified.

In some samples micas did not seem to form part of the primary mineral assemblage and were usually associated with opaque minerals and apatite (Fig. 6A). This was interpreted as caused by late crystallization. An example of this was sample G_2937, where two generations of biotite and muscovite were observed; the first formed part of the primary mineral assemblage, where the biotite was almost completely chloritized; the second generation was an accumulation of biotite and muscovite, where the biotites showed little to no alteration and had euhedral shapes (Fig. 6B, 8A). Three of the granitic intrusives (GV_2861, GV_3012, and GV_2815) were cut by quartz veins bordered with tourmaline crystals (samples GV_2815 and GV_2861) as seen in Figure 8B and 8C.

Pegmatites

These rocks (dykes, lenses, and Qz-rich rocks with pegmatitic texture) showed variable features both in composition and texture. Some of them had inequigranular texture between mesogranular and coarse, whereas others only had medium to thick crystals. The samples were divided into three groups according to their rock-forming minerals content (Qz-Plag-FK): (i) Rocks composed almost 100% of microcline and quartz in similar proportions, and without plagioclase: P_2807, P_2972, P_2995 and P_2940.
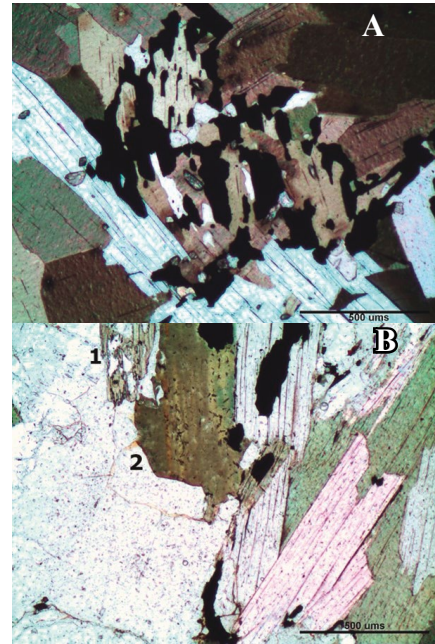

Figure 6. PPL microphotographs of granitic intrusives. (A) Sample G_2936 showing association between biotite and opaque minerals. (B) Sample G_2937 showing differential alteration of biotite (crystal 1 and 2).

(ii) Rocks composed of quartz between 75% and 95%, with low microcline content and without plagioclase P_2846, P_2883, P_3005, and P_2823.

(iii) Rocks composed of quartz, microcline, and plagioclase, with plagioclase content variable from predominant to in similar proportion with quartz and microcline, respectively: P_2917 (Fig. 7), P_2820 (Fig. 7), P_2870 and P_3006, P_2935, P_2984.
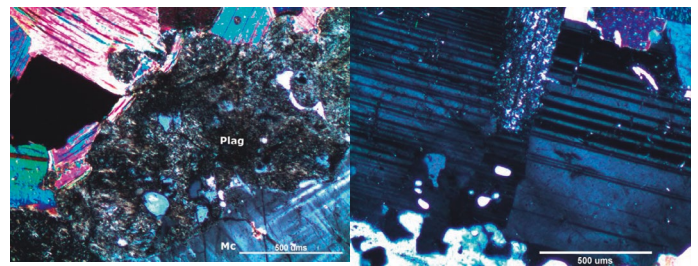

Figure 7. PPL microphotographs of pegmatites. Sample P_2917 (Left) showing highly altered plagioclase and no altered microcline (as in granitic intrusives). Sample P_2820 showing low alteration of plagioclase.

As accessory minerals for the three groups, muscovite, biotite, magnetite, and ilmenite were recognized. Nb-rutile was identified in samples P_2846 and P_2883. In sample P_3006 garnet was identified in association with muscovite.

Muscovite was common among the samples. In some of them biotite arranged in clusters and was associated with opaque minerals (as seen in the granitic intrusives, Fig. 6A), suggesting late biotite crystallization.

4.2 EPMA electronic microprobe analysis

4.2.1 Apatite

Eight points in five apatite crystals were analyzed from the granitic intrusives samples G_3003, G_2936, and G_2895 (representative photographs shown in Fig. 9); all crystals were associated with magnetite, ilmenite, and biotite. Regrettably, it was not possible to measure this mineral in all types of samples due to its scarcity.

Figure 8. Photographs of three thin sections (A) G_2937 showing an accumulation of dark minerals (biotite), (B) and (C) GV_2815 and GV_2861 respectively, show dark-colored minerals that correspond to tourmaline bordering quartz veinlets. The red circles show the location of the EPMA analyzed points.
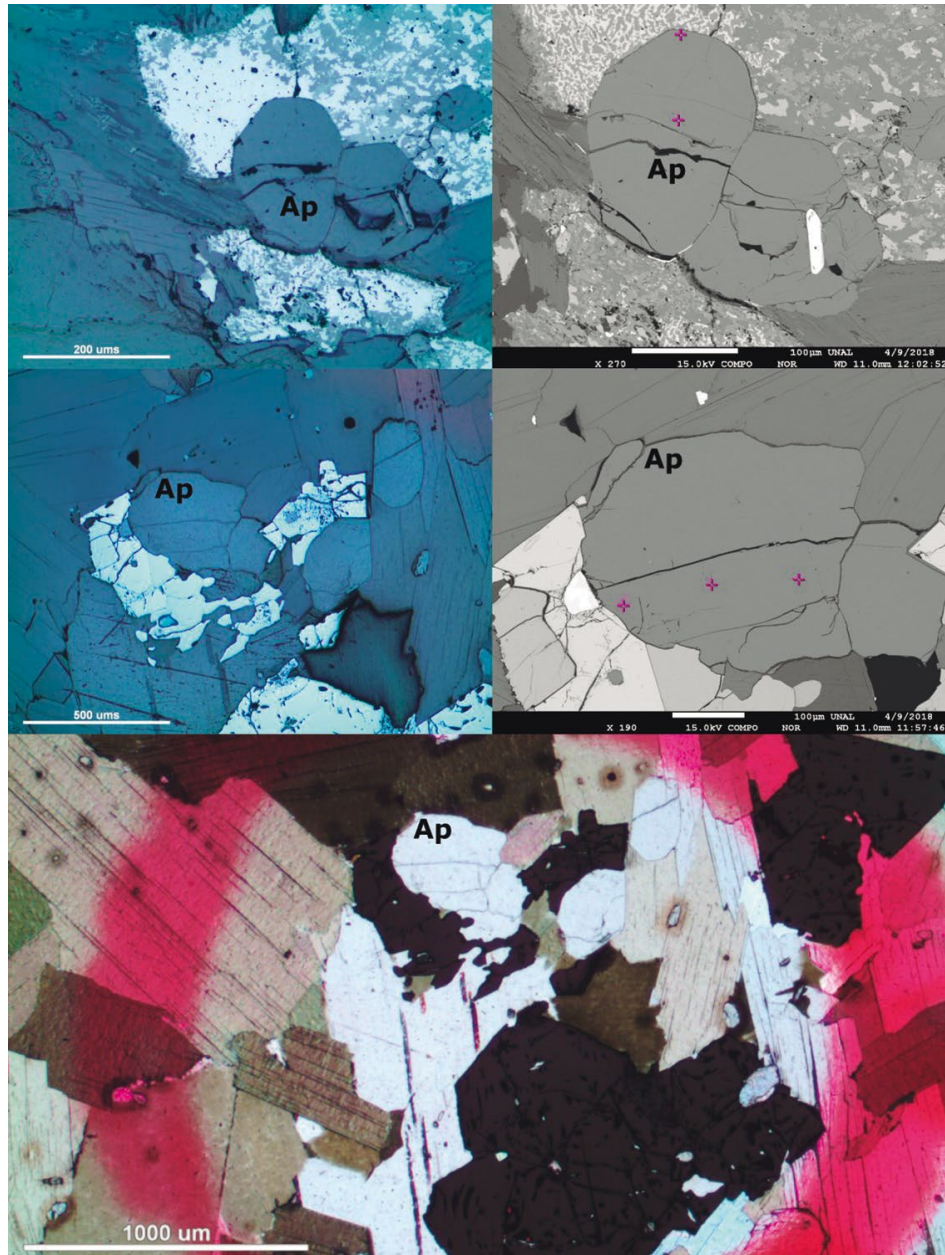

Figure 9. Representative images of analyzed apatites (Ap). The upper left and middle left images display polished thin section photographs from samples G_2895 and G_2936, respectively. These photographs showcase the association of apatites with magnetite and ilmenite. The upper right and middle right images present backscattered electron images of the analyzed crystals; the pink points represent the microprobe analyses conducted. The lower photograph, captured under plane-polarized light, exhibits the crystals surrounding the analyzed apatite. The association of micas with opaque minerals is shown.

The primary focus of the analysis of this mineral was the relationship between Sr and Mn as it is a marker of magmatic fractionation degree (Belousova et al., 2002); see Figure 10.
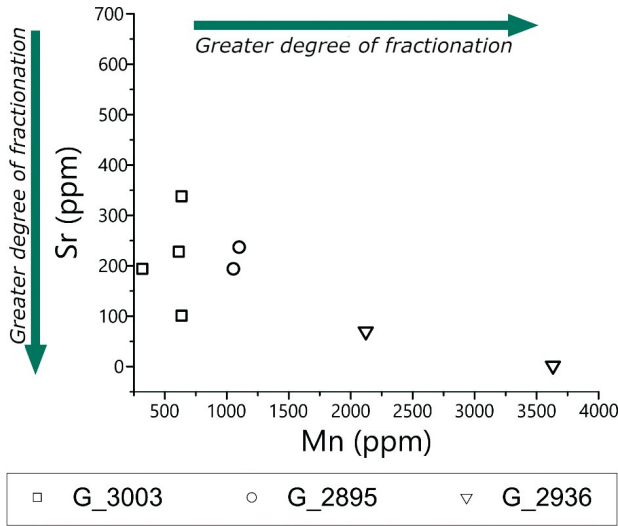

Figure 10. Sr vs Mn in apatite for the three analyzed granitic intrusives. Fractionation degree is shown according to Belousova et al. (2002).

Detailed weight percentages of major elements and ppm of trace elements (Si, Fe, Mn, Na, F, Cl, S, As, Sr, La, Ce, Nd) are shown in Appendix B1.

4.2.2 Biotite

Fourty-two points were analyzed in nineteen biotite crystals belonging to five granitic bodies (G_2973, G_3003, G_2936, G_2937, GV_3012), and three pegmatites (P_2972, P_2984, P_2870). Biotite crystals were found in other samples as well, but they were chloritized and thus not subjected to electronic microprobe analysis.

The Fe# was calculated for biotite (equation 1), since it is a marker of magmatic fractionation degree (Stussi & Cuney, 1996) (Fig. 11).
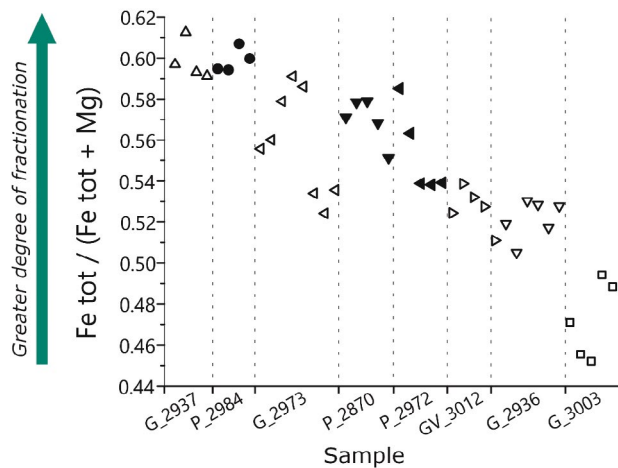
$$Fe\# = Fe_{tot} / (Fe_{tot} + Mg) \tag{1}$$

Figure 11. Fe# in biotite for samples of granites and pegmatites (filled symbols represent pegmatites while open symbols correspond to granitic intrusives). The samples are organized according to their fractionation degree, following Stussi & Cuney (1996).

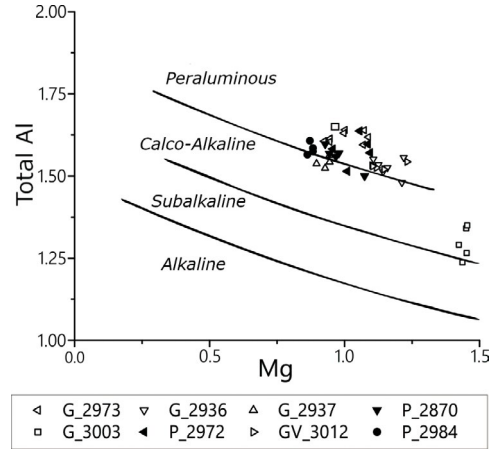Moreover, the Al vs Mg molar ratio was used to assess the magma type of the samples (Fig. 12).

Figure 12. Al vs Mg molar ratio in biotites. Magma type discrimination between peraluminous, calco-alkaline, subalkaline, and alkaline. Taken from Gomes and Neiva (2005) that modifies Nachit (1985).

Detailed compositional results are shown in Appendix B2.

4.2.3 Garnet

Three points in a single garnet crystal were analyzed from pegmatite P_3006 (Fig. 13), belonging to group iii. This crystal was found in association with muscovite.
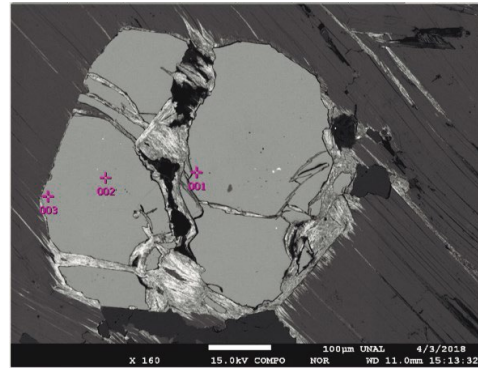

Figure 13. Backscattered electrons image of analyzed garnet crystal surrounded by muscovite (sample P_3006) with respective WDS measurement points in pink.

The composition of the garnet was predominantly spessartine with high content of almandine; moreover, the spessartine content rises from the center to the edge of the crystal, with a relative reduction of the other members (Fig. 14).
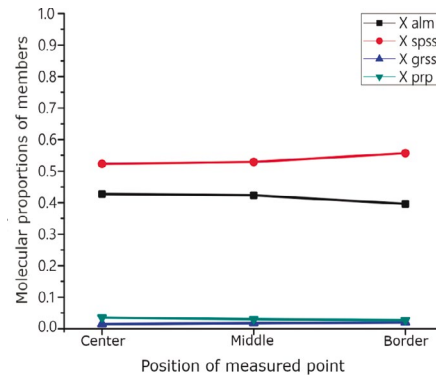

Figure 14. Composition of the garnet crystal in sample P_3006 in terms of almandine (alm), spessartine (spss), grossular (grss), and pyrope (prp).

For detailed compositional results refer to Appendix B3.

4.2.4 Microcline

Eighty-four points in thirty-one microcline crystals were analyzed. Eight crystals belonging to the group of granitic intrusives (GV_3012, GV_2861, G_3003, and G_2936), and the rest to pegmatites from group i, ii, and iii.

Ba, Pb, P, and Sr contents were obtained due to their suitability in showing increasing or decreasing fractionation degree trends of the host rock (Abad-Ortega et al., 1993; Alfonso et al., 2003; Černý et al., 1985; Kontak & Martin, 1997; London et al., 1990; Roda Robles et al., 1995).

However, in most cases, Sr concentration was close to the detection limit (Appendix B4), as obtained by Alfonso et al. (2003). Similarly, Pb and P were not useful to discriminate the samples according to their evolution degree due to high data dispersion (Fig. 15) and to very low concentrations among several samples.
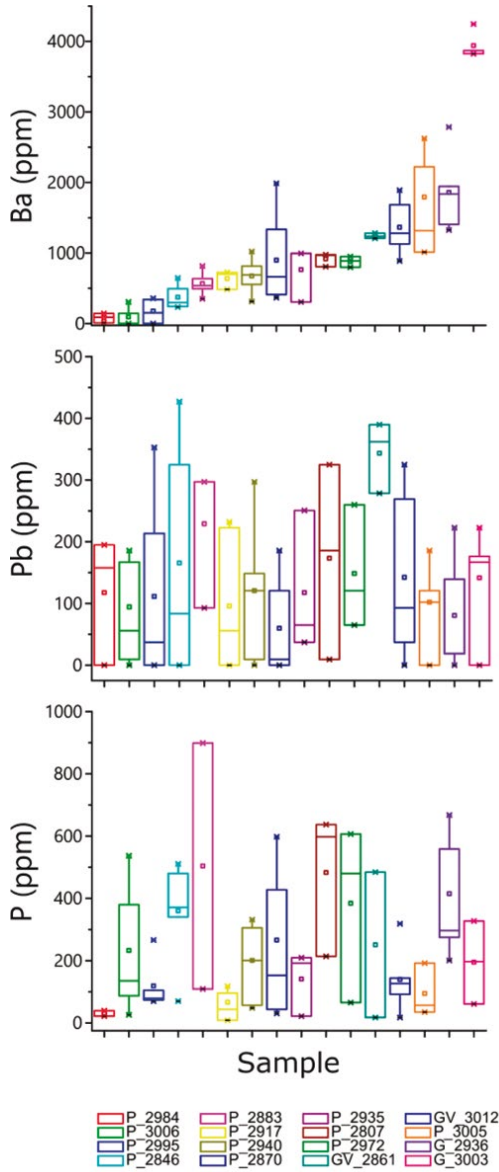

Figure 16. Ba concentration (ppm) in microcline for samples of granitic (open symbols) and pegmatitic intrusives (filled symbols) showing fractionation degree. The Nb-Ta-bearing samples (Bayona-Valderrama, 2018; Charry et al., 2023) are shown in red. Samples bearing garnet and tourmaline are marked.

4.2.5 Muscovite

Fifty-four points were analyzed from 23 crystals: six of them belonging to the granitic intrusives G_2936, GV_3012, GV_2861, and the remaining crystals belonging to pegmatites of the three groups. Ba, Na, Sn, Ti, W, Zn were measured (Fig. 17); according to Alfonso et al. (2003) these elements concentrate differentially in relation to fractionation degree.

Figure 15. Box and whisker plots for Ba, Pb, and P concentrations (top to bottom) in analyzed microcline samples.

Conversely, Ba presented low dispersion (Fig. 15), allowing the samples to be organized from lowest to highest Ba content and therefore, from highest to lowest fractionation degree (Černý et al., 1985; Roda Robles et al., 1995) (Fig. 16).
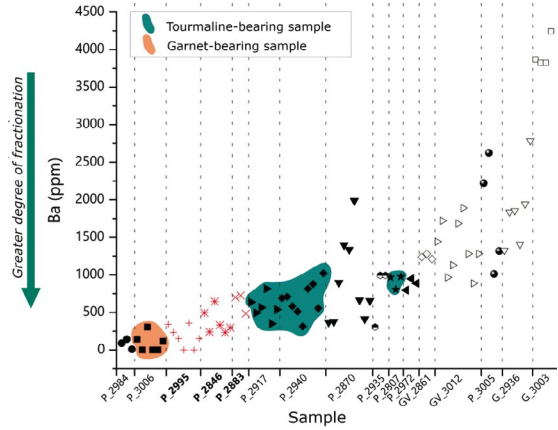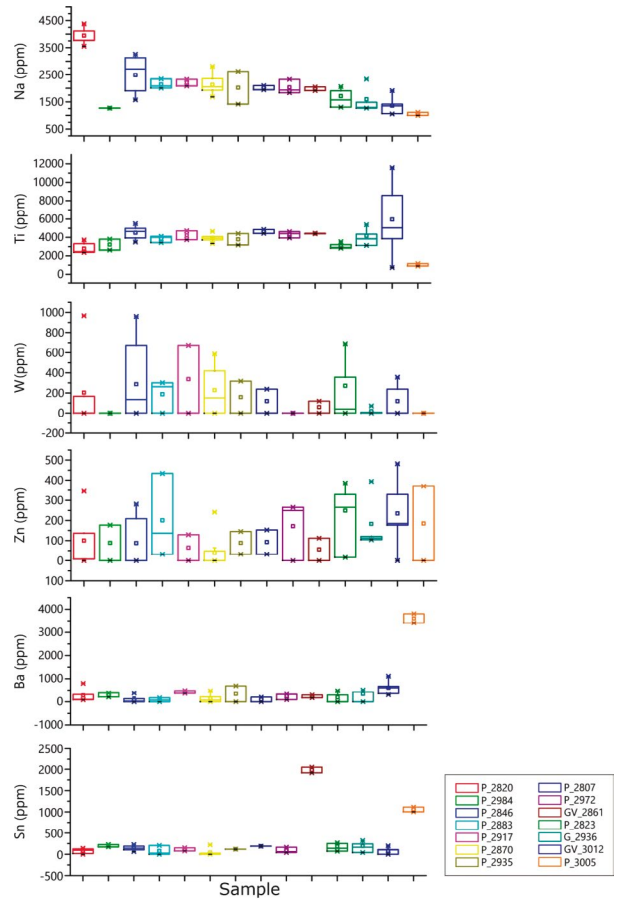
Figure 17. Box and whisker plots for the concentrations of Na, Ti, Ba, Sn, W, and Zn in the analyzed muscovites.

However, among these elements, the concentration of Na was the only that presented little dispersion and enough variability among samples (Fig. 17), allowing them to be sorted from highest to lowest concentration, and therefore, from highest to lowest fractionation degree (Alfonso et al., 2003) (Fig. 18).
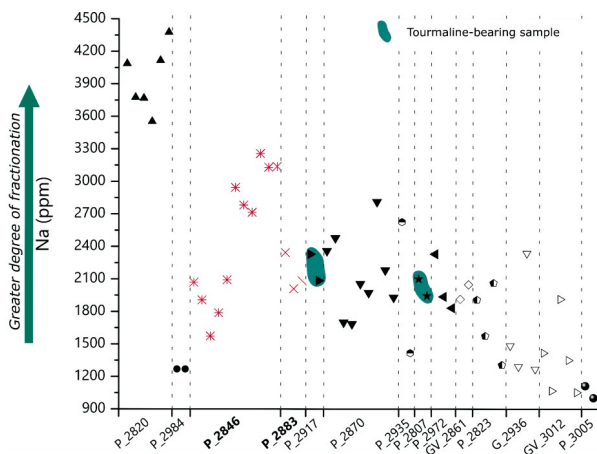

Figure 18. Na concentration (ppm) in muscovite for samples of granitic intrusives (open symbols) and pegmatites (filled symbols) showing fractionation degree. The samples bearing Nb-Ta minerals (Bayona-Valderrama, 2018; Charry et al., 2023) are shown in red.

Detailed compositional results are shown in Appendix B5.

4.2.6 Tourmaline

The chemical composition of 57 points of 13 crystals was analyzed. Out of these, three crystals belonged to paragneiss N_2816, five crystals were part of the tourmaline borders of the quartz veins that cut the granites GV_2861 and GV_2815, and five crystals belonged to pegmatites P_2917, P_2940 and P_2807 (see Appendix B6 for detailed composition). The cations calculation was made according to Henry & Guidotti (1985), assuming three boron atoms and obtaining the corresponding mass percentage to produce them (Appendix B6).

A compositional diagram was used following Henry and Guidotti (1985); accordingly, the analyzed rocks belong to "Fe^{+3}-rich granitic rocks" (Fig. 19). The crystals found in the paragneiss also fall into this classification indicating that these tourmalines might have crystallized during pegmatite emplacement (Morales et al., 2017).
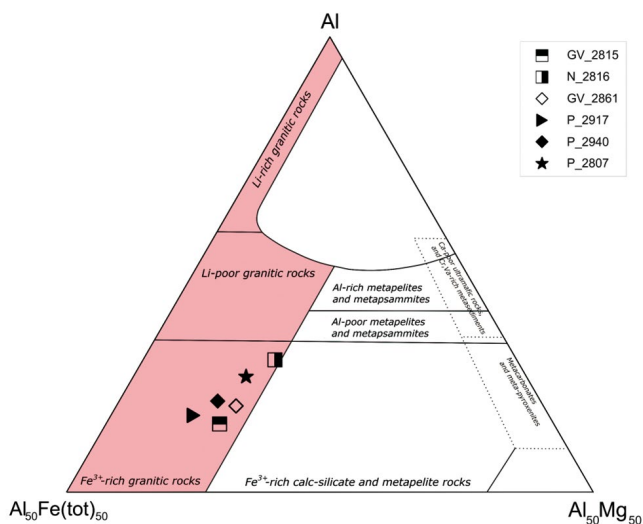

Figure 19. Al-Fe total-Mg (in molecular proportions) classification diagram based on quantitative tourmaline analysis. Modified from Henry and Guidotti (1985).

5. Discussion

5.1 Fractionation degree and relationship with Nb-Ta-bearing minerals

The analyses of apatite, biotite, microcline, and muscovite aimed to assess the fractionation degree of the rocks. Regarding the results from apatite and biotite, which mainly represented granitic intrusions and some pegmatites, not all granitic intrusives were in the same degree of fractionation (Figs. 10, 11), which can both indicate different intrusive generations or consecutive intrusions from an evolving single melt.

In addition, it would be expected that the pegmatitic bodies (where biotite was analyzed) showed a higher fractionation degree than the granitic intrusives if they belonged to the same petrogenetic evolution line. This can be seen in Figure 11 with two exceptions: (1) The granitic intrusive G_2937 appears as the most fractionated sample, above the pegmatite samples, which could be explained by the texture of biotite, which seemed to represent a later crystallization for this mineral compared to that of the rock, as exposed in Section 4.1 and shown in Figure 6A. (2) The granite G_2973 showed the greatest data dispersion, some of it being intermediate between two pegmatite bodies. Unlike in the previous sample, these biotite crystals do not show textural features that could indicate a more recent crystallization. Because of that, this intrusive might belong to a different magma generation, exhibiting a similar fractionation degree to the pegmatites from the other generation.

Moreover, results from both apatite and biotite (Figs. 10, 11) indicate that sample G_3003 was the least fractionated, and that sample G_2936 had a higher degree of fractionation than the first, confirming the results.

However, it is necessary to carry out chemical analysis on minerals that are present in as many samples as possible to understand the relationship between Nb-Ta-bearing minerals and the fractionation degree of the igneous bodies. Therefore, microcline and muscovite, found in almost all samples (Table 2), represent better petrogenetic evolution indicators than biotite and apatite for these samples.

According to the results of microcline, the pegmatite samples had the highest fractionation degree (Fig. 16). In turn, granitic intrusives contained the highest concentrations of Ba and thus were the least fractionated. This could denote a petrogenetic evolution line involving all the analyzed samples.

However, the pegmatite P_3005 appeared as one of the least fractionated (between granitic intrusives in this figure). Subsequently, this rock might come from a different magmatic source and does not seem to be associated with the evolutionary line that led to the other pegmatites and the Na-Ta-bearing minerals.

Furthermore, the location of the Nb-Ta-bearing samples on Figure 16 is consistent with the high magmatic fractionation degree that is required to concentrate incompatible elements to form independent mineral phases (Linnen et al., 2012). For this study, rocks bearing Nb-Ta-bearing minerals had microcline Ba concentrations lower than 699 ppm.

Despite the microprobe results, the presence of textural features related to pegmatite fractionation degree would be advantageous in the field. To this end, tourmaline and garnet presence in the samples were marked in Figure 16 and 18 showing a possible relation. Conversely, the mineralogical classification of pegmatites made in Section 4.1 did not show any relation to it.

It was inferred that tourmaline crystallization occurred in the early stages of Nb-Ta mineralization during the magmatic fractionation process, and garnet crystallized in advanced stages of fractionation. Therefore, the presence of these minerals is proposed as an exploration tool as they might indicate proximity to mineralized pegmatitic bodies.

Consequently, Ba concentration is suggested as an indicator of fractionation in pegmatitic bodies with similar characteristics in eastern Colombia, preferring it above Sr, P, and Pb contents.

Lastly, similarities were found between the results from Na in muscovite and those obtained with the analysis of Ba in microcline (Figs. 16, 18). First, pegmatites had the highest concentrations of Na, indicating a high fractionation degree (Alfonso et al., 2003), except for the pegmatite P_3005, which conforms to the results from microcline. In addition, the Nb-Ta-bearing pegmatites (Bayona-Valderrama, 2018; Charry et al., 2023) showed high magmatic fractionation degree (Fig. 18). Finally, samples with tourmaline showed a lower degree of petrogenetic evolution than the samples P_2846 and P_2883 (Nb-Ta

enriched), supporting the interpretation that this mineral crystallized in the early stages of Nb-Ta mineralization, as seen from microcline results.

However, some analyses did not concur with the data obtained from the microcline. In the case of sample P_2846 (Nb-Ta enriched), low Na contents contradict the approach of Linnen et al. (2012) which refers to the high magmatic fractionation degree necessary to concentrate Nb-Ta. For sample P_2984, the results do not coincide with the degree of fractionation given by the Ba in microcline.

In general, the order of samples relative to their fractionation degree coincides between the microcline and muscovite analyses supporting both results. The minor differences between both graphs may correspond to slight differences in crystallization time and the possible loss of Na in the muscovite given its mobile nature. Moreover, the fractionation degree line of the studied pegmatites evidenced a tight relationship with their host granites.

Considering the observed textural features in muscovite, and associated opaque minerals (such as those of economic interest), indicating a possible late crystallization (Section 4.1), one possible interpretation could be that these minerals formed in a different and posterior event than that of the pegmatites formation. However, this would lead to stochastic magmatic fractionation of the pegmatites (as shown by microcline) in relation to the presence of Nb-Ta-bearing minerals. Therefore, the texture of micas and iron, titanium, Nb-Ta oxides demonstrate that these were the last crystals to form in the pegmatites, rather than having formed in another event.

To conclude, Ba concentration in microcline is proposed as a better indicator of evolution than the concentration of Na in muscovite in the rocks of the region since Ba is a less mobile element than Na and due to the ubiquity and abundance of microcline in pegmatites and granitic intrusives of the area. In addition, as stated by Černý et al. (1985), K/Rb and K/Rb vs Cs analyses in microcline are great petrogenetic evolution markers and should be used in further studies.

5.2 Parental magma

The correlation of the granitic rocks from the Migmatitic Mitu Complex with other igneous bodies in the Rio Negro-Juruena Province would ease the exploration of strategic minerals; hence the significance to assess the magma type that originated the studied pegmatites and granitic bodies. For this aim, the results obtained from the chemical analysis of garnet, biotite, and tourmaline were analyzed.

The garnet presence in igneous rocks is usually restricted to granitoids and acidic volcanic rocks (Rene & Stelling, 2007). Its formation in these rocks can be caused by partial fusion occurring in the restitic phase (Allan and Clarke, 1981; Stone, 1988; Vennum and Meyer, 1979; White and Chappell, 1977), by high fractionation of a peraluminous melt under low-pressure conditions (Allan & Clarke, 1981; Hall, 1965; Harrison, 1988; Miller & Stoddard, 1981), or by the transportation of high-pressure phenocrysts up to the Earth's crust (Green, 1977; Rene & Stelling, 2007). Specifically, according to Manning (1983), the garnets found in pegmatites belong to the almandine-spessartine solid solution and are commonly Mn enriched.

The composition of garnet in sample P_3006 conforms with Manning's (1983) approach, since it was predominantly spessartine with high content of almandine (Fig. 14).

For this crystal, both being part of a restitic phase of a partial fusion process and being a phenocryst transported from high pressures to the crust were discarded for not conforming with the textural features observed in the field. Therefore, the formation from a highly fractionated peraluminous melt under low-pressure conditions (Allan & Clarke, 1981; Hall, 1965; Harrison, 1988; Miller & Stoddard, 1981) is supported by the obtained composition (Krippner et al., 2014).

The analysis of biotite confirmed this interpretation, as shown in Figure 12, where most of the samples correspond to peraluminous magmas, except for sample G_3003. The latter was the one showing the least evolution degree (Section 4.2) leading to the conclusion that this sample does not correspond to the petrogenetic line of the other samples as it comes from a different magma type.

Furthermore, the presence of biotite in the pegmatites, including those with a high degree of fractionation, may indicate high iron content in the source magma. This is supported by the composition of the tourmaline present in both pegmatites and the paragneiss sample, as shown in Section 4.2.6 and Figure 19.

In addition, according to Zen (1988), peraluminous igneous bodies can host incompatible elements such as Sn, W, and other lithophile elements such as U, Li, B, Ta, Nb, which is consistent with the presence of Nb-Ta-bearing minerals in the area (Bayona-Valderrama, 2018; Charry et al., 2023). According to Winter (2001), these magmas occur both in continental collision and post-orogenic tectonic environments. The studied rocks best relate to a post-orogenic tectonic environment according to Cardona-Alarcón (2018), who analyzed fluid inclusions of the tourmaline crystals (in paragenesis with plagioclase and microcline in the pegmatitic bodies) and found high content of CO_2 y N_2 with homogenization temperatures between 298,3-330ºC; the author concluded a mantellic origin for these rocks, discarding a continental collision environment. Accordingly, Franco et al. (2021b) analyzed colluvial REE, Nb–Ta, and U–Th bearing minerals in the Guainía Department (pegmatite-related) and concluded their relationship with intra-plate processes that produced anorogenic granites between 1.55 and 1.30 Ga, which can be related to plume activity. Furthermore, various reports of post-orogenic to anorogenic rocks in the vicinity of the study area have been made, several of which report the presence of strategic minerals (Bonilla et al., 2021; Bonilla et al., 2023; Cordani et al., 2016; Franco et al., 2021a; Franco et al., 2021b). Consequently, the studied rocks can be related to anorogenic intrusion events in the NW portion of the Rio Negro-Juruena Province such as that of the Matraca Granite or the Parguaza anorogenic event as reported for similar and neighboring igneous bodies (Aarden & Davidson, 1978; Bangerter, 1985; Bonilla-Perez et al., 2013; Bonilla et al., 2021; Bonilla et al., 2023; Franco et al., 2021a; Franco et al., 2021b; Gaudette et al., 1978; Gonzalez & Pinto, 1990; Rodriguez & Perez, 1982).

6. Conclusions

Microprobe chemical analysis on apatite, biotite, garnet, microcline, muscovite, and tourmaline revealed significant features of the studied igneous bodies, regarding their origin and petrogenetic evolution.

Garnet, biotite, and tourmaline composition indicated that pegmatites and most intrusive granites originated from iron-rich peraluminous magma Nb-Ta enrichment, and could be associated with neighboring anorogenic granitoids. Moreover, the studied bodies are compositionally associated with the host granites.

In addition, the assessment of the magmatic fractionation degree was achieved with the concentration of Na (ppm) in muscovite, Fe# in biotite, Sr vs Mn (ppm) in apatite, and Ba concentration (ppm) in microcline. The latter was the most effective due to its ubiquitous distribution and its low mobility; it should be further used in granites and pegmatites of this region in combination with K/Rb and K/Rb vs Cs analyses for their utility as petrogenetic evolution markers. The magmatic fractionation degree of the studied rocks was concordant with the presence of Nb-Ta-bearing minerals, such as columbite, Nb-rutile, and samarskite. The fractionation degree line of the studied pegmatites evidenced a tight relationship with their host granites.

In addition, tourmaline crystallized in early stages of Nb-Ta enrichment, while garnet crystallized in advanced stages of magma fractionation; therefore, these minerals are proposed as strategic mineral exploration tools in pegmatites of the region.

References

Aarden, H., & Davidson, M. (1978). *Minerales de estaño, niobio, tántalo y titanio en la zona del Cano Aguamena, Estado Bolívar, analizados con microsonda de electrones.* Congreso Geológico Venezolano, 5th, Memoria, 3. Caracas, pp. 919–940.

Abad-Ortega, M. M., Hach-Ali, P. F., Martin-Ramos, J. D., & Ortega-Huertas, M. (1993). The feldspars of the Sierra Albarrana granitic pegmatites, Cordoba, Spain. *The Canadian Mineralogist*, 31, 185–202.

Alfonso, P., Melgarejo, J. C., Yusta, I., & Velasco, F. (2003). Geochemistry of feldspars and muscovite in granitic pegmatite from the Cap De Creus Field, Catalonia, Spain. *The Canadian Mineralogist*, 41, 103–116. https://doi.org/10.2113/gscanmin.41.1.103

Allan, B. D., & Clarke, D. B. (1981). Occurrence and origin of garnets in the South Mountain batholith, Nova Scotia. *The Canadian Mineralogist*, 19, 19–24. DOI:10.1139/cjes-2016-0106

Andersen, T., & Neumann, E.-R. (2001). Fluid inclusions in mantle xenoliths. *Lithos 55,* 301–320. https://doi.org/10.1016/S0024-4937(00)00049-9

Bangerter, G. (1985). *Estudio sobre la Petrogenesis de las Mineralizaciones de Niobio, Tantalo y Estario en el Granito Rapakivi de Parguaza y sus Diferenciaciones*. Primer Simposio Amazónico, Puerto Ayacucho, Venezuela, pp. 175–185.

Barron, C. (1966). *Notes on the Stratigraphy of Central British of Guyana*. Conferencia Geologica Interguianas, 6. Departamento Nacional da Produqzo Mineral, Anais, BelCm, Pard, Brazil, pp. 121–126.

Bayona-Valderrama, J. P. (2018). *Análisis de espectros Raman en óxidos provenientes de áreas pegmatíticas en el oriente colombiano.* ［Unpublished manuscript].

Belousova, E. A., Griffin, W. L., O'Reilly, S. Y., & Fisher, N. I. (2002). Apatite as an indicator mineral for mineral exploration: Trace-element compositions and their relationships to host rock type. *Journal of Geochemical Exploration*, 76, 45–69. https://doi.org/10.1016/S0375-6742(02)00204-2

Belousova, E. A., Walters, S., Griffin, W. L., & O'Reilly, S. Y. (2001). Trace-element signatures of apatites in granitoids from the Mt Isa Inlier, Northwestern Queensland. *Australian Journal of Earth Sciences,* 48, 603–619. https://doi.org/10.1046/j.1440-0952.2001.00879.x

Bonilla, A., Cramer, T., De Grave, J., Alessio, B., Glorie, S., & Kroonenberg, S. (2021). The NW Amazonian Craton in Guainía and Vaupés departments, Colombia: Transition between orogenic to anorogenic environments during the Paleo-Mesoproterozoic. *Precambrian Research*, 360, 106223. https://doi.org/https://doi.org/10.1016/j.precamres.2021.106223

Bonilla-Pérez, A., Frantz, J. C., Charao-Marques, J., Cramer, T., Franco-Victoria, J. A., Mulocher, E., & Amaya-Perea, Z. (2013). Petrografía, geoquímica y geocronología del Granito de Parguaza en Colombia. *Boletín de Geología,* 35.

Bonilla, A., Franco-Victoria, J. A., Cramer, T., Grave, J. de, Nachtergaele, S., Cogné, N., & Piraquive, A. (2023). The NW Amazonian Craton in Guainía and Vaupés departments, Colombia: Evidence of a Mesoproterozoic thermal event from Apatite LA-ICP-MS U-Pb geochronology and its relation to magmatic ore deposits. Precambrian Research, 395(July), Manuscript Number: PRECAM-D-23-00131. https://doi.org/10.1016/j.precamres.2023.107148

Brito Neves, B. B. (2011). The Paleoproterozoic in the South-American continent: Diversity in the geologic time. *Journal of South American Earth Sciences,* 32, 270–286. https://doi.org/10.1016/j.jsames.2011.02.004

Cardona Alarcón, A. C. (2018). *Caracterización microtermométrica de fluidos mineralizantes en diques pegmatíticos en el oriente colombiano*. [Unpublished Manuscript] Bogotá, Colombia.

Černý, P. (1994). Evolution of Feldspars in Granitic Pegmatites. In: Parsons, I. (eds) *Feldspars and their Reactions*. NATO ASI Series, vol. 421. Springer, Dordrecht. https://doi.org/10.1007/978-94-011-1106-5_13

Černý, P., Meintzer, R. E., & Anderson, A. J. (1985). Extreme fractionation in rare-element granitic pegmatites; selected examples of data and mechanisms. *The Canadian Mineralogist,* 23, 381–421.

Charry, C. J., Molano, J. C., Santacruz, L. and Sepulveda, J. (2023). Magnetic Petrology applied to the characterization of Pegmatite Dykes in Eastern Colombia. *Earth Sciences Research Journal*, 27(1), 11–25. https://doi.org/10.15446/esrj.v27n1.102683

Cordani, U. G., Sato, K., Sproessner, W., & Fernandes, F. S. (2016). U-Pb zircon ages of rocks from the Amazonas Territory of Colombia and their bearing on the tectonic history of the NW sector of the Amazonian Craton. *Brazilian Journal of Geology*, https://doi.org/10.1590/2317-4889201620150012

Franco, J. A., Cramer, T., Bonilla, A., Castañeda A. J., Poujol, M., & Amaya, Z. (2021). Mineralogía y geocronología de rutilo-(Nb,Ta) relacionado a casiterita y columbita-tantalita provenientes de rocas Mesoproterozoicas del Cratón Amazónico cerca de Cachicamo, Colombia. *Boletín de Geología*, 43(1), 99-126. https://doi.org/10.18273/revbol.v43n1-2021005

Franco, J. A., Cramer, T., Chaves, A. de O., Horn, H. A., & Poujol, M. (2021). Geochronology of monazite related to REE, Nb–Ta and U–Th bearing minerals from Mesoproterozoic anorogenic magmatism in the E-Colombian Amazonian Craton: Links to mantle plume activity in the Columbia (Nuna) supercontinent. *Journal of South American Earth Sciences*, 109, 103228. https://doi.org/https://doi.org/10.1016/j.jsames.2021.103228

Gaudette, H. E., Mendoza, V., Hurley, P. M., & Fairbairn, H. W. (1978). Geology and age of the Parguaza rapakivi granite, Venezuela. *Bulletin of the Geological Society of America,* 89, 1335–1340. https://doi.org/10.1130/0016-7606(1978)89<1335:GAAOTP>2.0.CO;2

Gomes, M. E. P., & Neiva, A. M. R. (2005). Geochemistry of granitoids and their minerals from Rebordelo – Agrochao area, northern Portugal. *Lithos 81,* 235–254. https://doi.org/10.1016/j.lithos.2004.11.001

Gonzalez, C. F., & Pinto, H. (1990). Petrografia del Granito de Parguaza y otras Rocas Precambricas en el Oriente de Colombia. *Geología Colombiana, 17,* 107–121.

Green, T. H. (1977). Garnet in silicic liquids and its possible use as a P-T indicator. *Contributions to Mineralogy and Petrology,* 65, 59–67. https://doi.org/10.1007/BF00373571

Guerrero, N., Santacruz, L., Dorado, C., Rodriguez, B., Morales, M., Cano, N., Martínez, L., Zárate, A., Molano, J., Peña, G., & Perez, A. (2017). *Caracterización de pegmatitas al sureste del departamento de Guainía, Colombia*. XVI Congreso Colombiano de Geología, III Simposio de Exploradores, Santa Marta, Colombia, pp. 1267–1272.

Hall, A. (1965). The Origin of Accessory Garnet in the Donegal Granite. *Mineralogical Magazine, 35*, 628–633. https://doi.org/10.1180/minmag.1965.035.272.06

Harrison, T. N. (1988). Magmatic Garnets in the Cairngorm Granite, Scotland. *Mineralogical Magazine,* 52, 659–667. https://doi.org/10.1180/minmag.1988.052.368.10

Henry, D. J., & Guidotti, C. V. (1985). Tourmaline as a petrogenetic indicator mineral: an example from the staurolite-grade metapelites of NW Maine. *American Mineral*ogist, 70, 1–15.

Kontak, D. J., & Martin, R. F. (1997). Alkali feldspar in the peraluminous South Mountain Batholith, Nova Scotia: Trace-element data. *The Canadian Mineralogist*, 35, 959–977.

Krippner, A., Meinhold, G., Morton, A. C., & Von Eynatten, H. (2014). Evaluation of garnet discrimination diagrams using geochemical data of garnets derived from various host rocks. *Sedimentary Geology,* 306. https://doi.org/10.1016/j.sedgeo.2014.03.004

Linnen, R. L., Van Lichtervelde, M., & Černý, P. (2012). Granitic pegmatites as sources of strategic metals. *Elements, 8*, 275–280. https://doi.org/10.2113/gselements.8.4.275

London, D., Cerny, P., Loomis, J. L., & Pan, J. J. (1990). Phosphorus in Alkali Feldspars of Rare-Element Granitic Pegmatites. *The Canadian Mineralogist,* 28, 771–786.

López, J., Khurama, S., Bernal, L., & Cuellar, M. (2007). El Complejo Mitú: Una Nueva Perspectiva. *Memorias XI Congreso Colombiano de Geología,* 1–16.

López, J. A., & Cramer, T. (2014). Ambiente Geológico Del Complejo Mitú Y Tantalio En El Territorio Colombiano Geological Setting of Mitu Complex and Perspective of Mineral Occurrences of Niobium and Tantalum in the Colombian Territory. *Geología Colombiana,* 37, 75–93.

Manning, D. A. C. (1983). Chemical variation in garnets from aplites and pegmatites, peninsular Thailand. *Mineralogical Magazine,* 47. https://doi.org/10.1180/minmag.1983.047.344.10

Miller, C. F., & Stoddard, E. F. (1981). The Role of Manganese in the Paragenesis of Magmatic Garnet: An Example from the Old Woman-Piute Range, California. *The Journal of Geology,* 89, 233–246. https://doi.org/10.1086/628582

Morales, M., Santacruz, L., Molano, J., Dorado, C., Zárate, A., Rodriguez, B., Guerrero, N., Cano, N., Martínez, L., Perez, A., & Peña, G. (2017). *Consideraciones sobre la fuente de Nb y Ta en el departamento del Guainía: un abordaje desde el fluido y la química mineral.* XVI Congreso Colombiano de Geología, III Simposio de Exploradores*, pp. 1052–1057.*

Nachit, H. (1985). Composition chimique des biotites et typologie magmatique des granitoids. *Comptes Rendus de l'Académie des Sciences,* 301, 813–818.

Pan, Y., & Fleet, M. E. (2002). Compositions of the Apatite-Group Minerals: Substitution Mechanisms and Controlling Factors. *Reviews in Mineralogy and Geochemistry,* 48, 13–49. https://doi.org/10.2138/rmg.2002.48.2

Piccoli, P. M., & Candela, P. A. (2002). Apatite in Igneous Systems. *Reviews in Mineralogy and Geochemistry,* 48, 255–292. https://doi.org/10.2138/rmg.2002.48.6

Priem, H. N. A., Andriessen, P. A. M., Boelrijk, N. A. I. M., De Boorder, H., Hebeda, E. H., Huguett, A., Verdurmen, E. A. T., & Verschure, R. H. (1982). Geochronology of the Precambrian in the Amazonas Region of Southeastern Colombia (Western Guiana Shield). *Geologie en Mijnbouw,* 61, 229–242.

René, M., & Stelling, J. (2007). Garnet-bearing granite from the Třebíč pluton, Bohemian Massif (Czech Republic). *Mineralogy and Petrology,* 91, 55–69. https://doi.org/10.1007/s00710-007-0188-2

Roda Robles, E., Pesquera Peréz, A., & Velasco Roldán, F. (1995). Micas of the muscovite-lepidolite series from the fregeneda pegmatites (Salamanca, Spain). *Mineralogy and Petrology,* 55, 145–157. https://doi.org/10.1007/BF01162585

Rodríguez, G., Sepúlveda, J., Ramírez, C., Ortiz, F., Ramos, K., Bermúdez, J., & Sierra, M. (2011). Cartografía Geológica y Exploración Geoquímica de la Plancha 443 Mitú. 163.

Rodríguez, S., & Pérez, H. (1982). Nb, Ta, and Sn mineralization related to granitic magmatism in western Bolivar State, Venezuela: International Association on the Genesis of Ore Deposits. *Symposium, 6th, Tbilisi, U.S.S.R.* p. 10p.

Santos, J. O. S., Rizzotto, G. J., Potter, P. E., McNaughton, N. J., Matos, R. S., Hartmann, L. A., Chemale, F., & Quadros, M. E. S. (2008). Age and autochthonous evolution of the Sunsás Orogen in West Amazon Craton based on mapping and U-Pb geochronology. *Precambrian Research,* 165, 120–152. https://doi.org/10.1016/j.precamres.2008.06.009

Sha, L. K., & Chappell, B. W. (1999). Apatite chemical composition, determined by electron microprobe and laser-ablation inductively coupled plasma mass spectrometry, as a probe into granite petrogenesis. *Geochimica et Cosmochimica Acta,* 63, 3861–3881. https://doi.org/10.1016/S0016-7037(99)00210-0

Shearer, C. K., Papike, J. J., & Laul, J. C. (1985). Chemistry of potassium feldspars from three zoned pegmatites, Black Hills, South Dakota: Implications concerning pegmatite evolution. *Geochimica et Cosmochimica Acta,* 49, 663–673. https://doi.org/10.1016/0016-7037(85)90161-9

Stone, M. (1988). The Significance of Almandine Garnets in the Lundy and Dartmoor Granites. *Mineralogical Magazine,* 52, 651–658. https://doi.org/10.1180/minmag.1988.052.368.09

Stussi, J., & Cuney, M. (1996). Nature of Biotites from Alkaline, Caloalkaline and Peraluminous Magmas by Abdel-Fattah M. Abdel-Rahman: A Comment. *Journal of Petroleum,* 37, 1025–1029. https://doi.org/10.1093/petrology/37.5.1025

Tassinari, C. C. G., & Macambira, M. J. B. (1999). Geochronological provinces of the Amazonian Craton. *Episodes 22*, 174–182. https://doi.org/10.18814/epiiugs/1999/v22i3/004

Teiber, H., Marks, M. A. W., Arzamastsev, A. A., Wenzel, T., & Markl, G. (2015). Compositional variation in apatite from various host rocks: clues with regards to source composition and crystallization conditions. *Neues Jahrbuch für Mineralogie - Abhandlungen - Journal of Mineralogy and Geochemistry,* 192, 151–167. doi:10.1127/njma/2015/0277

Vennum, W. R., & Meyer, C. E. (1979). Plutonic garnets from the Werner Batholith, Lassiter Coast, Antarctic Peninsula. *American Mineralogist,* 64, 268–273.

White, A. J. R., & Chappell, B. W. (1977). Ultrametamorphism and granitoid genesis. *Tectonophysics 43,* 7–22. https://doi.org/10.1016/0040-1951(77)90003-8

Winter, J. D. (2001). *An Introduction to Igneous and Metamorphic Petrology.* Prentice-Hall Inc.

Zárate, A., Morales, M., Santacruz, L., Guerrero, N., Molano, J., Dorado, C., Peña, G., Perez, A., Amaya, Z., Franco, J., Rodríguez, B., Cano, N., Martínez, L., & Molano, J. (2017). *Caracterización de granos de ilmenorutilo en concentrados de batea utilizando diferentes métodos analíticos. Sureste del departamento de Guainía, Colombia.* XVI Congreso Colombiano de Geología, III Simposio de Exploradores, pp. 1058–1064.

Zen, E. (1988). Phase relations of peraluminous granitic rocks and their petrogenetic implications. *Annual Review of Earth and Planetary Sciences,* 21–51.